



Pilot scale cellulose recovery from sewage sludge and reuse in building and construction material



Silvia Palmieri^a, Giulia Cipolletta^{a,*}, Carlo Pastore^b, Chiara Giosuè^a, Çağrı Akyol^c, Anna Laura Eusebi^{a,*}, Nicola Frison^d, Francesca Tittarelli^{a,e}, Francesco Fatone^a

^a Department of Science and Engineering of Materials, Environment and Urban Planning-SIMAU, Marche Polytechnic University, Ancona 60131, Italy

^b Water Research Institute, National Research Council (IRSA-CNR), Bari 70132, Italy

^c Institute of Environmental Sciences, Boğaziçi University, 34342 Istanbul, Turkey

^d Department of Biotechnology, University of Verona, Verona 37129, Italy

^e Institute of Atmospheric Sciences and Climate, National Research Council (ISAC-CNR), Bologna 40129, Italy

ARTICLE INFO

Article history:

Received 10 February 2019

Revised 18 August 2019

Accepted 10 September 2019

Keywords:

Sewage wastes valorisation

Toilet paper

Cellulosic sludge

Construction industry

Recovered material

ABSTRACT

The recovery of cellulose in toilet paper from municipal wastewater is one of the most innovative actions in the circular economy context. In fact, fibres could address possible new uses in the building sector as reinforcing components in binder-based materials. In this paper, rotating belt filters were tested to enhance the recovery of sludge rich in cellulose fibres for possible valorisation in construction applications. Recovered cellulosic material reached value up to 26.6 gm⁻³ with maximum solids removal of 74%. Content of cellulose, hemicellulose and lignin was found averagely equal to 87% of the total composition. Predictive equation of cellulosic material was further obtained. The addition of recovered cellulose fibres in mortars bring benefits in terms of lightness, microstructure and moisture buffering value (0.17 g/m²%UR). Concerning mechanical properties, flexural strength was improved with the addition of 20% of recovered cellulose fibres. In addition, a simplified economic assessment was reported for two possible pre-mixed blends with 5% and 20% of recovered fibres content.

© 2019 Elsevier Ltd. All rights reserved.

1. Introduction

In recent years, circular economy approach has been developing in different industrial sectors to achieve sustainable production processes and to reduce consumption of resources. Similarly, the technologies in the water cycle treatment and management have been evolving towards this direction that focus more on the valorisation of the final wastes (Schreck and Wagner, 2017; Silva et al., 2017; Crutchik et al., 2018; Akyol et al., 2019). Cellulosic material in the toilet paper, which is the major organic component in the urban influent that enters the municipal treatment plants (Ruiken et al., 2013), holds a great potential as one of the most recoverable products from wastewater flows.

In general, the potential recovery of cellulose is closely linked to the daily use of toilet paper. This consumption is extremely variable, heterogeneous and closely related to the degrees of urbanization, sanitation, sewage infrastructures and waste transport. For these reasons, the potential recovery has to be referred to specific

territorial scale. In fact, variable ranges of data are reported in the scientific literature, equal to 49 ± 23 g toilet paper p⁻¹d⁻¹ in America, to 31 ± 21 g toilet paper p⁻¹d⁻¹ in Europe, to 5 g toilet paper p⁻¹d⁻¹ in Asia and to 1 g toilet paper p⁻¹d⁻¹ in Africa (Toilet Paper History, 2018; Matter of Scale, 2018; Southeast Green, 2018). Assuming that toilet paper contains approximately 85% of cellulosic compounds (Industrial Shredders, 2018), the maximum potential recovery of cellulose varies from 42 g toilet paper p⁻¹d⁻¹, in the most industrialized countries, to 1 g toilet paper p⁻¹d⁻¹ in developing countries.

In this scenario, several research activities and European projects have focused on the recovery of resources from wastewaters (Pioneer_STP, SMART-Plant (smart-plant.eu), INCOVER (incover.eu), Res Urbis (resurbis.eu), Screencap (screencap.eu)). Specifically, projects such as Screencap, Pioneer and SMART-Plant, have implemented the recovery of cellulosic fraction in wastewater treatment plants (WWTPs) through the integration of the dynamic separation technology into conventional treatment flow schemes. This unit easily allows to separate a greater fraction of solids and to retain the cellulose fibres more efficiently while replacing the traditional primary sedimentation (Ruiken et al., 2013). The separated material; on the other hand, needs to be industrially washed and dried

* Corresponding authors.

E-mail addresses: g.cipolletta@univpm.it (G. Cipolletta), a.l.eusebi@univpm.it (A.L. Eusebi).

Nomenclature

C_{Ycell}	Cellulosic Yield Coefficient	R_c	Compressive Strength
COD	Chemical Oxygen Demand	R_f	Flexural Strength
CP	Pure Cellulose Fibres	REF	Mortar Without Cellulose Fibres Addition
CREC	Recovered Cellulose Fibres	RH	Relative Humidity
CRIC	Recycled Cellulose Fibres	SEM	Scanning Electron Microscope
E%TSS	Percentage of the Separation Efficiencies based on total suspended solids removal	SLR	Solids Loading Rate
EDAX	Energy Dispersive X-ray	SSD	Saturated Surface Dry
H_{min}	Minimum Hydraulic Level	T	Temperature
H_{max}	Maximum Hydraulic Level	TS	Total Solids
HLR	Hydraulic Loading Rate	TVS	Total Volatile Solids
IAQ	Indoor Air Quality	TSS	Total Suspended Solids
ITZ	Interfacial Transition Zone	V_{total}	Volume of Flask
M_{fibres}	Quantity of SSD fibres	V_{water}	Volume of Distilled Water
MBC	Moisture Buffering Capacity	WVP	Water Vapour Permeability
MBV	Moisture Buffering Value	WWTP	Wastewater Treatment Plant
MIP	Mercury Intrusion Porosimetry	Y_{cell}	Specific Cellulosic Material Production
PE	Population Equivalent	ρ	Density
Q	Flow rate	δa	Vapour Permeability of Stagnant Air
RBF	Rotating Belt Filtration	δp	Vapour Permeability of the Material
		μ	Water Vapour Diffusion Resistance Factor

to extract the recovered cellulose fibre. Therefore, the optimization of the cellulose separation in the WWTPs could enable the enhancement of the recovery of this product in the water sector as well as in other industrial manufacturing fields (Jeihanipour et al., 2010; Shi et al., 2018; Hietala et al., 2018; Zhang et al., 2018).

Cellulosic fibres have already been investigated in engineering applications as a reinforcing component in binder-based materials (Huber et al., 2011; Huber et al., 2014; Ardanuy et al., 2015). They give beneficial properties to mortars/concretes in terms of mechanical characteristics and the ability to improve indoor comfort with less environmental impact compared to metallic or plastic fibres.

However, the building sector consumes about 40% of the global energy mainly for the production of mortars and concretes (Dittenber and Gangarao, 2012). Therefore, a significant increase in sustainability of mortars/concretes production can be achieved by replacing virgin raw materials with renewable and/or so-called “waste ones” (Dittenber and Gangarao, 2012; Wei et al., 2013; Giosuè et al., 2017). Although recovered cellulose fibres from other industrial activities are often used in the building engineering applications (Andrés et al., 2015), the cellulose recovered from municipal wastewater have never been considered until now. In particular, recycled cellulosic waste paper fibres are already commercially available as insulation material and cement composites reinforced with recycled cellulosic waste paper fibres have been already investigated in the literature (Ashori et al., 2011; Hospodarova et al., 2018). Differently, cellulose recovered from real municipal wastewater treatment has not been considered yet.

Therefore, this paper aims to investigate the possibility of cellulose recovery from municipal wastewater and its valorisation in the building sector. Specifically, the recovery of cellulose fibres was carried out by enhanced primary separation in demonstrative pilot plants that were installed in two real municipal WWTPs. The effect of the addition of recovered cellulosic fibres at different percentages on the properties of hydraulic lime-based mortars was tested for non-structural applications. The properties of mortars that were manufactured with the same dosages of pure cellulose fibres and of recycled cellulose from newspaper were further compared. Finally, technical feasibility and economic considerations were discussed to promote the valorisation of recovered cellulose and its economic assessment in the building sector.

2. Methods

2.1. Dynamic separation: Demonstrative scale applications

The potential recovery of cellulose was studied in 2 WWTPs located in Falconara Marittima and Carbonera, Italy. The Falconara WWTP treats wastewater from a combined sewer system for average capacity of 29,000 m³d⁻¹ with nominal size of 81,000 PE. The Carbonera WWTP has nominal dimension of 40,000 PE and the average flow rate in dry period, mainly from separated sewer systems, is equal to 14,400 m³d⁻¹.

In Falconara WWTP, a demonstrative system of dynamic filtration (Salsnes SF 1000 by Trojan Technologies) was installed and fed by the effluent from the pre-treatment section (degripping and desanding units) of the full-scale plant. The influent flow rate to the filter was assured by one external pump (Pedrollo F4-65/200AR) that works in the range of 15 m³h⁻¹–78 m³h⁻¹. The flow rate was regulated by manual valve and controlled by Krohne NSF-61-G flowmeter. A mixing storage tank (MST1) of 1 m³ of volume was placed before the dynamic filter. The cellulosic sludge and the effluent flow were separated by the filter and collected in two different tanks before being discharged to the main WWTP (MST2 and MST3). Two online total solids (TS) probes (Lange P/n LXG 423.99.00100) were installed in MST1 and MST3 for the continuous measurement of solids concentration during the separation tests.

In Carbonera WWTP, the effluent after the pre-treatment units (degripping and oil removal) was sent to mixing storage tank (1 m³ of volume) and to the following rotating filter (Salsnes SF 1000 by Trojan Technologies) in the same configuration of Falconara site. A centrifugal pump (Flygt N 3085.160) was installed to feed the filter and controlled by an inverter to adjust the influent flow rate. The flowmeter (NSF-61-4 Krohne) continuously measured the influent of the rotating unit. Water tanks were also provided in both pilot plants for the cleaning of rotating belt filter (RBF). The cleaning operation was carried out before and after each separation test, by volumetric water pump at minimum temperature of 70 °C.

The separated cellulosic sludge and effluent flow were stored in different tanks to be sampled and characterized before the discharge. The characterization of the influent and effluent in both

sites was carried out according to Standard Methods for the Examination of Water and Wastewater (APHA/AWWA/WEF, 2012). Moreover, the determination of the influent granulometric distribution of the wastewater in the Falconara WWTP was conducted in laboratory scale by the sieving method (Van Loosdrecht et al., 2016).

Different sets of experiments were performed for the separation of cellulosic sludge (21 in Falconara WWTP and 14 in Carbonera WWTP). Accordingly, varying operating parameters were applied to investigate their influence on the solids separation yields. The duration of the tests was between 1 h and 14.5 h with an average duration of 4 h in each test. Specifically, the influent flow rate was set to $15 \text{ m}^3\text{h}^{-1}$ (in 2 tests-F1, F2), $30 \text{ m}^3\text{h}^{-1}$ (in 21 tests - F3-F10, F12, F13, F15, F16, F19, F20, C8-C14), $40 \text{ m}^3\text{h}^{-1}$ (in 7 tests C1-C7) and $50 \text{ m}^3\text{h}^{-1}$ (in 5 tests F11, F14, F17, F18, F2). To study the effect of the filtration surface increment during the 35 tests, the minimum (H_{\min}) and maximum (H_{\max}) hydraulic levels in the filtration chamber were ranged from 75 mm to 260 mm, as reported in Table 2. In each test, the obtained performances in terms of total suspended solids (TSS) removal were related to the hydraulic loading rate (HLR) ($\text{m}^3 \text{ h}^{-1}$ for m^2 of filtration area) and to the solids loading rate (SLR) (kg TSS h^{-1} for m^2 of filtration area). Finally, different belts with porosities from $90 \mu\text{m}$ to $350 \mu\text{m}$ were used in the Falconara pilot plant, and only the mesh at $350 \mu\text{m}$ was installed in Carbonera pilot during the experimental period.

2.2. Cellulosic sludge recovery optimization and model prediction

The separated sludges were analyzed to determine the cellulosic material content. The matrices (tests F4-5, F8, F9, F11, F14-16, F19-21) were first sieved at $63 \mu\text{m}$ and washed with tap water in laboratory scale for 30 min according to (Ruiken et al., 2013). The procedure allowed to obtain sludge devoid of the finest aggregates and more concentrated in cellulose fibres. These samples were then analysed to determine the percentages of proteins, lipids, ashes, hemicellulose, pure cellulose, lignin and humic compounds according to analytical method reported by (Di Bitonto et al., 2016). Gas-chromatographic analyses were performed by using a Varian 3800 (GC-FID) equipped with a MDN-5S capillary column (30 m; 0.25 mm , $0.25 \mu\text{m}$ film). Fatty acid methyl esters were quantified by using methyl heptadecanoate as internal standard. Sugars were qualitatively and quantitatively determined by using a GS50 chromatography system Dionex-Thermo Fisher Scientific.

For the determination of the cellulosic material recovery yield, the cellulosic yield coefficient $C_{Y_{\text{cell}}}$ was expressed according to Eq. (1):

$$C_{Y_{\text{cell}}} = \frac{gTVS_{\text{Post}} - \text{Washing}}{gTSP_{\text{Pre}} - \text{Washing}} \quad (1)$$

where:

g TVS = the amount of the total volatile solids in the sludge separated from the WWTP post-washing;

g TS = the amount of the total solids in the sludge separated from the WWTP pre-washing.

With this coefficient the specific cellulosic material production (Y_{cell}) was calculated by Eq. (2):

$$Y_{\text{cell}} = \left(\frac{gTSP_{\text{Pre}} - \text{Washing}}{\text{m}^3} \cdot C_{Y_{\text{cell}}} \right) \cdot \frac{(\%_{\text{cellulose}} + \%_{\text{hemicellulose}} + \%_{\text{lignin}})}{100} \quad (2)$$

where:

g TS m^{-3} = the concentration of the total solids in the sludge separated from the WWTP pre-washing;

$\%_{\text{cellulose}}$, $\%_{\text{hemicellulose}}$, $\%_{\text{lignin}}$ = percentages of cellulose, hemicellulose and lignin analysed in the sludge separated from pilot plant.

In the literature, several models correlated the removal of TSS with the influent solids for dynamic separation unit (Behera et al., 2018). The solids removal efficiencies of this study were plotted with the influent solids concentrations and compared to the previous models to evaluate the fitting behaviour of the experimental data. Moreover, predictive equation was found that links the solid removal performances ($E\%TSS$) in the rotating belt filtration with the potential cellulose recovery as expressed in Eq. (2) (Y_{cell}).

2.3. Implementation of recovered cellulose in the building sector

The recovered cellulosic fibres from wastewater (CREC) was added in hydraulic lime based mortars to investigate their possible valorisation in the building sector. Different mortar mix designs were compared both by adding increasing dosages of CREC fibres and by using pure fibres (CP) and by recycled ones (CRIC) from newspapers in the same proportions.

2.3.1. Fibres characterization

Considering the elevated amount of cellulosic material to be used in the mortar's tests, the CREC fibres were provided by CirTec BV. CirTec BV is a partner of SMART-Plant Project (smart-plant.eu) and its core business is the recovery of cellulosic fibres from WWTPs using RBF units in industrial scale with the same configuration of the demonstrative plants of Falconara and Carbonera.

CP (Arbocel B400) and CRIC (Arbocel ZC900) fibres were provided by J. RETTENMAIER & SOHNE (JRS). CP and CRIC fibres were chosen specifically by length comparable to CREC ones.

The fibres were morphologically investigated by a Scanning Electron Microscope (SEM-EDAX) (ZEISS 1530-Carl Zeiss, Oberkochen, Germany) equipped with a Schottky emitter.

The estimation of the amount of water absorbed by cellulose fibres to reach the Saturated Surface Dry (SSD) to elaborate the mix-design was obtained according to the procedure of (Gómez Hoyos et al., 2013).

To measure apparent density, a certain quantity of SSD fibres (M_{fibres}) was inserted into a flask in triplicates. The flask ($V_{\text{total}} 50 \text{ ml}$) was refilled with distilled water (V_{water}) and weighted to obtain the final density values.

2.3.2. Mortars mix design and characterization

Mortars were manufactured with a water/binder = 0.63 and an aggregate/binder = 3 by weight using a commercial hydraulic lime (NHL5), according to EN 459-1:2010, as binder (Ardanuy et al., 2015; Válek et al., 2014; Lucas et al., 2013) and a calcareous sand (98% of CaCO_3 , $d_{\max} = 400 \mu\text{m}$ and density of 2.65 g cm^{-3}) (Triantafyllou et al., 2011) provided by "Cava Gola della Rossa" (Ancona-IT) as aggregate.

Fibres were added in the mortar mix by 0% (REF), 5%, 10%, 15% and 20% by mortar volume (Jongvisuttisun et al., 2013; Hospodarova et al., 2018). NHL5 was initially mixed with sand and cellulose to obtain a homogeneous matrix, and water was subsequently added and the blend and mixed for 3 min. In all mixes, aggregate and fibres were added in SSD conditions according to UNI EN 1015-11:2007.

To investigate the effect of different fibres addition on the fresh properties of mortars, the workability was evaluated by the slump flow test using a truncated cone (100 mm base diameter, 70 mm top diameter, and 60 mm height) according to UNI EN 1015-3:2007.

The morphology of mortars was investigated by Scanning Electron Microscope (SEM) to compare macroscopic properties with microstructure. Moreover, the total pore volume and the pore size

distribution of different mixes were measured by Mercury Intrusion Porosimetry (MIP) (Thermo Fisher, Pascal series 240).

After 28 days of curing, the density (ρ , in g dm^{-3}) of hardened mortars was calculated according to UNI EN1015-11:2007. Compressive and flexural strength (R_c and R_f) tests were carried out on at least three prisms ($40 \text{ mm} \times 40 \text{ mm} \times 160 \text{ mm}$) according to the Italian standard UNI EN1015-11:2007.

2.3.3. Hygrometric behaviour: Water vapour permeability and moisture buffering capacity

Water vapour permeability measurements were carried out according to the UNI EN 1015-19:2007 to assess the water vapour transfer and humidity storage capacities of mortars as reported previously (Collet et al., 2008; Collet and Pretot, 2012; Maslinda et al., 2017; Wang et al., 2000). The obtained data were further processed according to UNI EN ISO 12572:2007. The average results of the test are reported in terms of the water vapour diffusion resistance factor, μ . μ is defined as the ratio between the vapour permeability of stagnant air δ_a (kg (Pams)^{-1}) and the vapour permeability of the material δ_p (kg (Pams)^{-1}) at the same temperature and pressure (Slanina and Šilarová, 2009). Furthermore, if applied as renders in indoor applications, these mortars also have the potential to improve indoor microclimate and consequently the comfort and health of occupants (Khedari et al., 2001; Osanyintola and Simonson, 2006; Tran Le et al., 2010). The mortars manufactured in this study (based on cellulose fibres) could therefore influence the Indoor Air Quality (IAQ) positively in terms of water vapour permeability (Mazhoud et al., 2016) and moisture buffering capacity (MBC) (Gonçalves et al., 2014; Hospodarova et al., 2018). The moisture buffering value (MBV) quantifies the capacity of a material to absorb and release moisture from/to the environment where it is placed (Rode et al., 2007). In this paper, the influence of cellulose fibres on MBV of mortars was assessed by a simplified version of the NORDTEST method (Abadie and Mendonça, 2009) where specimens were cyclically exposed to different RHs (Relative Humidity) for fixed periods.

The exposure to different RHs was carried out by placing the specimens inside two boxes containing a saturated solution of magnesium chloride (MgCl_2 , RH = 33%) and sodium chloride (NaCl, RH = 75%), respectively. The boxes were kept inside a climatic chamber to maintain the temperature constant at 20 ± 2 °C. Four cycles were carried out. The amount of water vapour absorbed or released by the specimens during each step was determined by measuring the weight of the specimens before changing boxes. The practical MBV ($\text{g (m}^2 \text{ RH)}^{-1}$) was calculated as the amount of moisture changed by the material per surface unit and RH gradient (Giosuè et al., 2017).

3. Results and discussion

3.1. Performances of dynamic separation and effects of the implementation in the WWTP

The results on the influent flows of Falconara and Carbonera WWTPs were analyzed to determine the optimal RBF conditions. In Falconara WWTP, the average concentrations of TSS and COD were detected as $112 \pm 82 \text{ mg TSS L}^{-1}$ and to $192 \pm 140 \text{ mg O}_2 \text{ L}^{-1}$, respectively. These values are typical for the plants located near the coastal area and characterized by contributions of seawaters intrusions (Conductivity $1432 \pm 96 \mu\text{S cm}^{-1}$) mainly during the wet periods. Meanwhile, in Carbonera WWTP, the influent was characterized by more elevated concentrations of solids and carbon loads with an average of $219 \pm 119 \text{ mg TSS L}^{-1}$ and $444 \pm 191 \text{ mg O}_2 \text{ L}^{-1}$, respectively.

An initial granulometric distribution test was carried out on the influent of Falconara. The results showed that the percentage of the influent TSS lower than $90 \mu\text{m}$ was equal to 82% and only 6% of the TSS had size between 90 and $250 \mu\text{m}$.

The obtained separation efficiencies from the dynamic filtrations in the pilot plants of Falconara and Carbonera varied between 11% and 75%. The results of the separation tests revealed that different factors could influence the separation yields. Firstly, improvements in separation yields were achievable using a lower porosity of the RBF. In fact, efficiencies increased from $37 \pm 19\%$ for mesh at $350 \mu\text{m}$ to $74 \pm 2\%$ for mesh at $90 \mu\text{m}$.

However, mesh size is not the only parameter that influences the separation yields positively. Therefore, the solids removals in the pilot plants were related to the specific SLR ($\text{kg TSS m}^{-2} \text{h}^{-1}$) (Fig. 1). In fact, even by using the same belt mesh, highest removal efficiencies were achieved with respect to elevated SLRs. Specifically, the optimal operating SLR varied between $25 \text{ kg TSS m}^{-2} \text{h}^{-1}$ and $40 \text{ kg TSS m}^{-2} \text{h}^{-1}$. For values higher than $40 \text{ kg TSS m}^{-2} \text{h}^{-1}$ up to $108 \text{ kg TSS m}^{-2} \text{h}^{-1}$, an increase of SLR did not origin the proportional increment of solids removal (E%TSS).

The increase of SLR corresponded to water level and the influent TSS variation in the filtration chamber that was related to the increase of the cake over the belt. This mechanism paved the way to remove even the fractions smaller than $90 \mu\text{m}$ (minimum nominal size of produced belt for Salsnes SF 1000) and to obtain removal efficiencies up to 70%. In fact, the formation of a particulate material layer on the belt surface caused a “fouling effect” on the filtration area (Franchi and Santoro, 2015) and improved the filtration efficiencies.

The separated effect of the flow rate and solids concentration (TSS_{IN}) on the E%TSS values was further investigated. The experimental tests showed that the influent TSS concentrations were more influential on the separation efficiencies than the flow rate. In fact, the filter ability of the system was automatically adjusted by changing the belt speed when the influent flow rate increased (Franchi and Santoro, 2015).

The solids removal trend of Falconara and Carbonera tests was fitted on the basis of the influent TSS and further compared to the literature models. The obtained separation efficiencies thoroughly reflected the Behera model of 2018 (Behera et al., 2018). Moreover, the hydraulic levels also influenced the solids removal efficiencies. Particularly, the results of the separation tests (F9, F11, F12, F14, F15, F17, F19, F21) with hydraulic depths ($H_{\text{max}} - H_{\text{min}}$) fixed at 260 mm (H_{max}) and 240 mm (H_{min}) showed a lower average removal efficiency ($48 \pm 22\%$) compared to tests (F10, F13, F16, F18, F20) at 220 mm of H_{max} and 200 mm of H_{min} (E%TSS averagely equal to $57 \pm 17\%$). The results could be attributed to the thinner layer of particles accumulated on the belt during the filtration cycle when higher hydraulic levels were set. This phenomenon is particularly enhanced when modest solids load is distributed on the filtration surface area as in the case of Falconara (Franchi and Santoro, 2015). This result identified the minimization of the water level upstream the filter setting lower set-points values ($H_{\text{max}} - H_{\text{min}}$) as possible control strategy to achieve an increment in TSS removal efficiencies.

3.2. Separation yields and cellulose recovery

The average content of cellulosic material in the separated solids was analysed in different experimental tests. The specific partitions in the sludge samples showed that the separated fraction by the RBF ranged between 6%–14% for lipids (on average 10%), 2%–28% for ashes (on average 15%), 6%–8% for hemicellulose (on average of 7%), 17%–39% for pure cellulose (on average 28%) and 23%–29% for lignin and humic compounds (on average 26%).

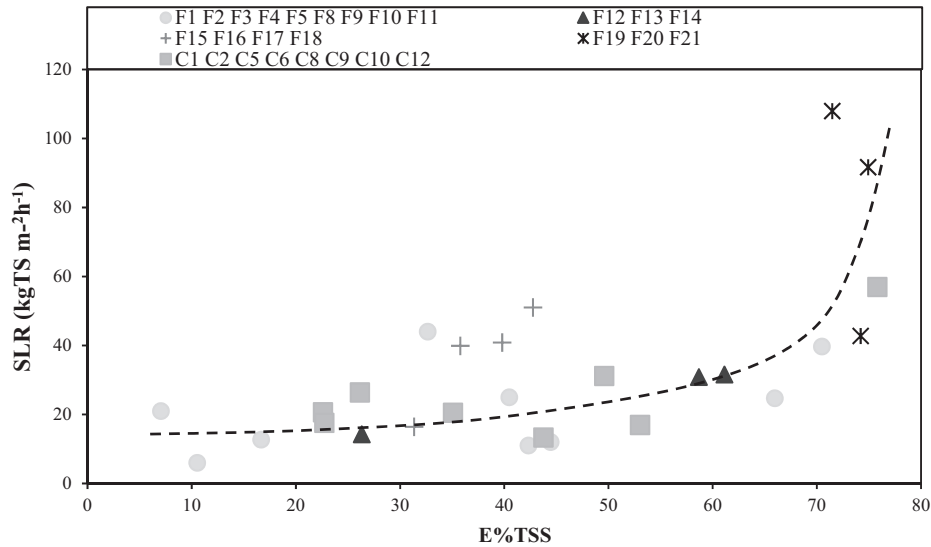


Fig. 1. Solid Loading Rates and TSS Removal Efficiencies of Falconara and Carbonera Pilot Plants- with different influent flow rates of (a) F1, F2 = 15 m³h⁻¹; (b) F3, F4, F5, F8, F9, F10, F12, F13, F15, F16, F17, F18, F19, F20, F21, C8, C9, C10, C12 = 30 m³h⁻¹; (c) C1, C2, C5, C6 = 40 m³h⁻¹; (d) F11, F14, F17, F18 = 50 m³h⁻¹.

Finally, approximately 12% of protein and 2% of other compounds were detected in the samples.

Moreover, after the wash of cellulosic sludge, small portion of lipids and fine inert solids as well as almost all the protein content were removed. Therefore, the final cellulosic materials showed more constant composition and were averagely characterized by 9% ± 1% of lipids; 6 ± 1% of ashes; 9 ± 1% of hemicellulose; 38 ± 6% of pure cellulose; 40 ± 3% of lignin and humic compounds; 0% of protein and other compounds.

According to Eq. (1), the cellulosic yield coefficient ($C_{Y_{cell}}$) was calculated for washed sludge samples. The average value of the coefficient was equal to 0.83 ± 0.14 g cellulosic material (g TS)⁻¹. Then, according to Eq. (2), with values of $C_{Y_{cell}}$ the specific cellulosic material productions (Y_{cell}) were determined for each test. Specific cellulosic material productions increased with respect to the solids removal efficiencies reaching up to 26.6 g cellulosic material m⁻³ (average of 7.82 ± 6.87 g cellulosic material m⁻³).

Fig. 2 illustrates the data of potential sum of cellulose, hemicellulose and lignin recovery from the cellulosic sludge linked to TSS removal efficiencies. The average concentrations of cellulosic material were equal to 15.9 ± 10.1 g m⁻³ (with values up to 26.6 g m⁻³) with filtration on belt at 90 μm, to 4.9 ± 4.5 g m⁻³ (up to 8.1 g m⁻³) with the 150 μm filter mesh, to 4.9 ± 2.0 g m⁻³ (up to 7.2 g m⁻³) with the mesh at 250 μm and to 5.9 ± 4.4 g m⁻³ (up to 11.4 g m⁻³) with mesh of 350 μm. The yields obtained with

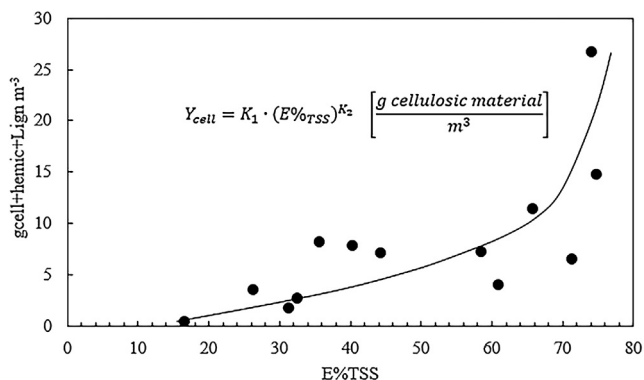


Fig. 2. Cellulosic Material Recovery and TSS removals.

mesh of 90 μm were averagely 3 times higher than those achieved with other meshes as shown in Fig. 2. Moreover, belts with meshes of 150 μm, 250 μm and 350 μm did not lead to significant differences of cellulosic materials recovery.

Although the length of the fibres did not change during transport in the sewer network (Ruiken et al., 2013), the reason for the higher recovery with 90 μm mesh could be attributed not only to the concentration of organic volatile solids (TVS) (average of 15.9 g m⁻³) separated during filtration tests but also to the quality of the organic solid component in the wastewater, such as the presence of fibrous material. In fact, thanks to their shape, fibrous structures (like cellulose) in the organic fraction can easily adhere to the surface of the belt and thus enhance the formation of the thick and porous filtration layer on top of the filtration area. (Franchi and Santoro, 2015). This filter mat, together with a low belt mesh, could consequently enhance the removal efficiencies of TSS and organics.

The average percentages of cellulose, hemicellulose and lignin were used to evaluate the recovery of cellulosic material, expressed as Y_{cell} , and to model a prediction equation of recovery. The solid separation efficiencies were therefore compared to the value of recovery of cellulosic material present in the organic fraction of cellulosic sludge (Fig. 2).

The predictive equation of the potential recovery and the experimental factors K_1 and K_2 were further reported (Eq. (3)) by linking the innovative way the solids removal and the potential cellulosic compounds to be valorized in the building sector.

$$Y_{cell} = K_1 \cdot (E\%_{TSS})^{K_2} \left[\frac{g_{cellulosic\ material}}{m^3} \right] \quad (3)$$

$$\text{With } K_1 = 0.0041, K_2 = 1.8845 \text{ and } R^2 = 0.71$$

3.3. Implementation of recovered cellulose in the building sector

3.3.1. Fibres characterization

The nominal lengths of CP and CRIC fibres (900 μm) were chosen similar to CREC one (1000 μm). The length of CREC was measured according to the same methodology reported by (Abadie and Mendonça, 2009). The similar lengths distributions were confirmed by microscope and statistical analysis (Fig. 3-g).

The morphological aspect and the diameters distribution (Fig. 3) of the different types of fibres were observed by SEM. The

surfaces of CRIC and CREC fibres appeared rougher than that of CP fibres. CRIC showed ribbon form; whereas CP and CREC were characterized by more tubular shape. In terms of diameters (Fig. 3-h), CP ($d_{\text{average}} = 11.6 \mu\text{m}$) and CREC ($d_{\text{average}} = 11.1 \mu\text{m}$) appeared finer than CRIC ($d_{\text{average}} = 13.0 \mu\text{m}$) (Fig. 3-e). Therefore, the aspect ratio (length/diameter) of CREC fibres seemed higher than that of CP and CRIC fibres. Moreover, the statistical distribution of CP and CREC diameters was less broad compared to CRIC (Fig. 3-e).

To reach the SSD condition, the water absorption was higher in CREC (119%) than in CP and CRIC (63% and 78%, respectively) fibres, probably due to their lower wettability and micro-fibril aggregation induced by the previous submitted processes, as discussed in Section 3.3.2. Apparent densities of 0.47 g cm^{-3} and 0.46 g cm^{-3} were measured for CP and CREC, respectively; whereas it was measured as 0.39 g cm^{-3} for CRIC.

3.3.2. Mortars mix design

3.3.2.1. Characterization and functional test. The Mix Designs of different mortars and the corresponding slump values are reported in Table 1.

The addition of fibres generally decreased the workability of mortars (Kawashima and Shah, 2011), similar to this case.

However, despite small differences in fibres microstructure (Fig. 3), all mortars remained to the same workability class equal to stiff (according to UNI EN 1015-6:2007) (Table 1).

In mortars, agglomerates of fibres may form; however, SEM observations of mortars showed a good dispersion of cellulose fibres, regardless their origin (Table 2). Moreover, more particles of binder paste were present on the surface of CREC fibres, than in CP and CRIC fibres. More adhered paste particles suggested a better adherence between fibres and matrix. This aspect determined a better Interfacial Transition Zone (ITZ) as shown in Table 2 where the limit between fibres and paste resulted less evident than in other mortars.

The best adherence of CREC fibres to the binder paste could be due to their rougher surface as observed in Fig. 3. Moreover, in CRIC fibres the pulping method induced irreversible structural changes by reducing the hemicellulose and lignin content (Oksanen et al., 1997; Wistara and Young, 1999). Hemicellulose consists of highly hydrophilic polysaccharide chains, which are usually the main contributor to water absorption (Fan and Fu, 2016). Therefore, the wetting ability, plasticity, ductility, stiffness and tensile strength of fibres also decrease by collapsing into ribbons and flocks (Howard and Bichard, 1992).

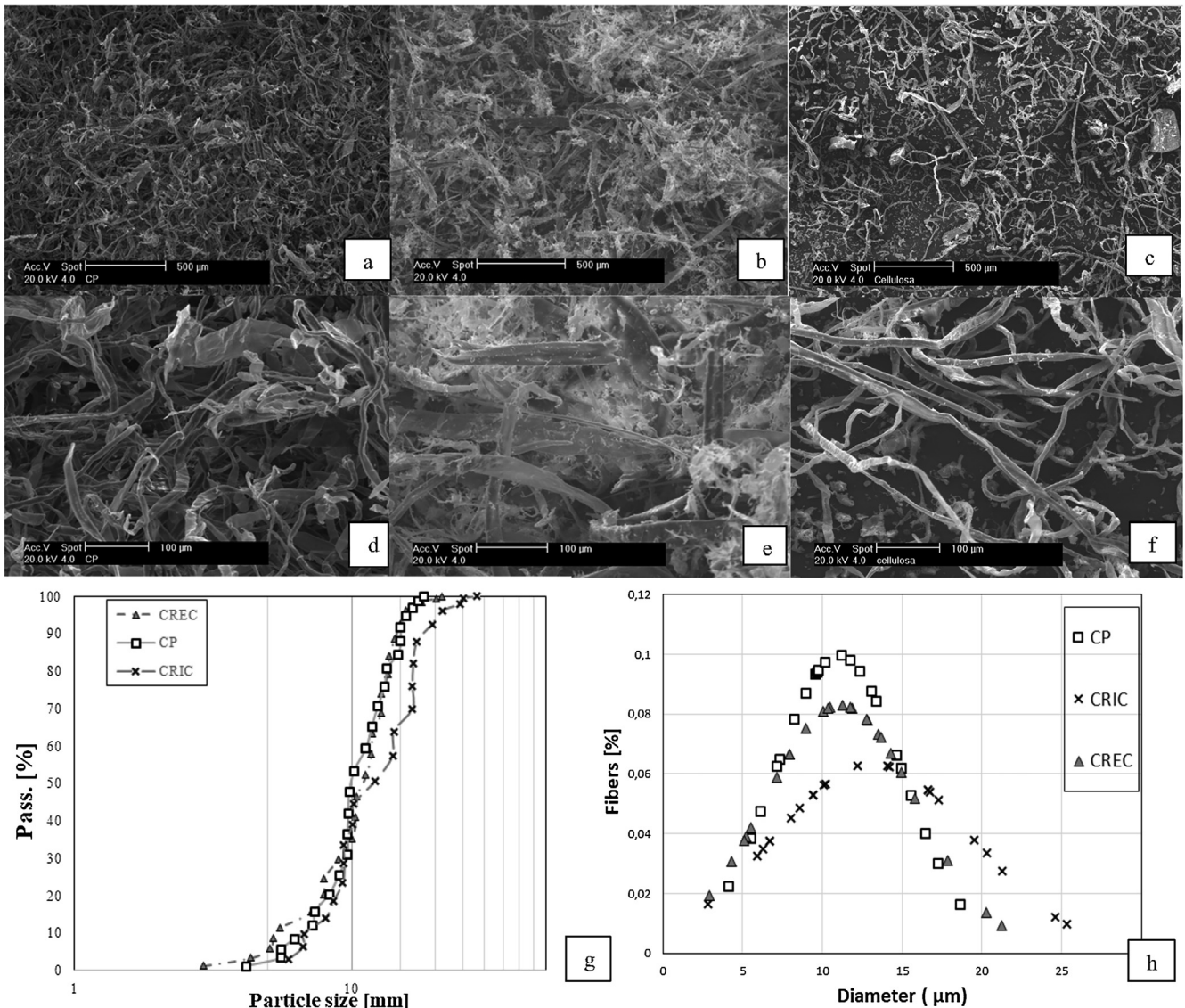
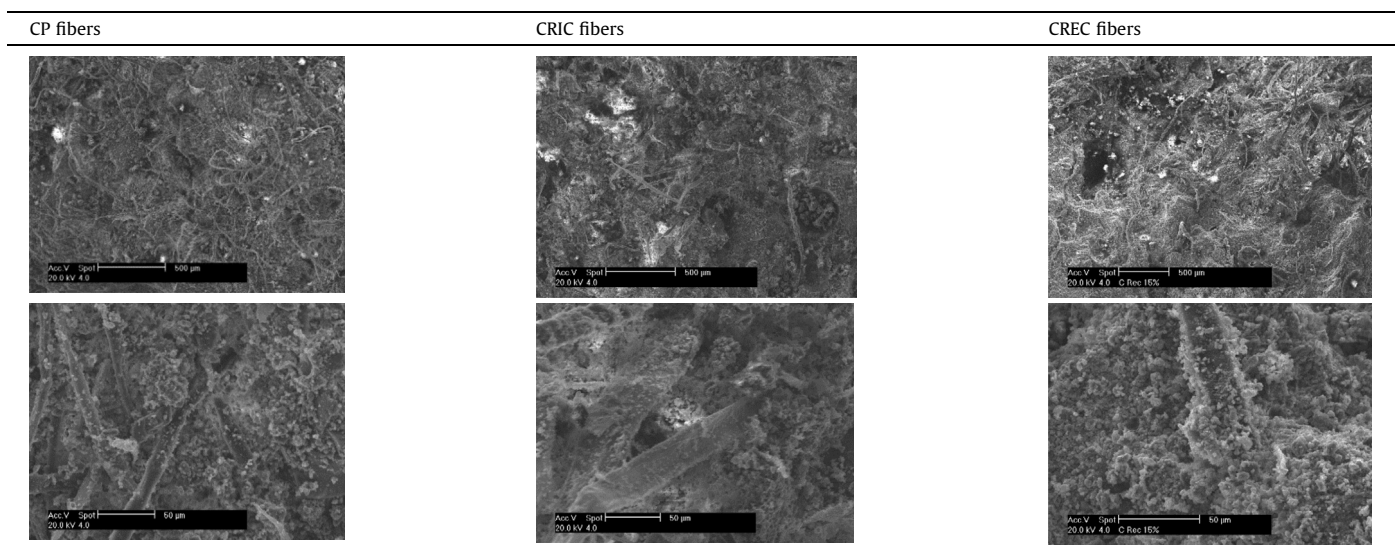


Fig. 3. (a) CP fibers; (b) CRIC fibers; (c) CREC fibers; (d) CP fibers enlargement (e) CRIC fibers enlargement; (f) CREC fibers enlargement; (g) Lengths distribution of CP, CRIC and CREC fibres and (h) Diameters distribution of CP, CRIC and CREC fibres.

Table 1
Mix Design (g/L) and slump values of different mortars.

		Water	NHL5	CA400	CP	CRIC	CREC	Slump (cm)
Reference	g	295	467	1402	0	0	0	118
CP 5%	g	281	445	1335	22	0	0	118
CRIC 5%	g	281	445	1335	0	19	0	117
CREC 5%	g	281	445	1335	0	0	22	117
CP 10%	g	268	425	1274	43	0	0	108
CRIC 10%	g	268	425	1274	0	35	0	115
CREC 10%	g	268	425	1274	0	0	42	115
CP 15%	g	256	406	1219	61	0	0	108
CRIC 15%	g	256	406	1219	0	51	0	107
CREC 15%	g	256	406	1219	0	0	60	111
CP 20%	g	246	389	1168	78	0	0	107
CRIC 20%	g	246	389	1168	0	65	0	111
CREC 20%	g	246	389	1168	0	0	77	109

Table 2
SEM observation of mortars with 20% addition of different fibers.



Higher amount of cellulose fibres caused higher presence of pores and an increase in their diameters in mortars. Specifically, the total accessible porosity increased from 31% (REF) to 34% (CREC 20%), 36% (CP 20%) and 37% (CRIC 20%). Whereas the REF mortar showed a unimodal pore size distribution, mortars with fibres had a bi-modal pore size distribution with the second peak moving to bigger pores, especially for CRIC, as reported in Fig. 4. This result was due to the porous structure of added cellulosic fibers and the additional porosity of the ITZ between fibers and binder paste (Savastano and Agopyan, 1999). This is true especially for CRIC mortars where the ITZ is more porous due to the bed adherence of CRIC fibers to the binder paste (Table 2), caused by the pulping method which decreases the fibers wetting ability, as reported above.

As expected, an increased addition of fibres, the lightest ingredient of the mortars, increased the porosity and reduced the binder paste content, that further caused a reduction in density, as reported in Fig. 5-a.

Consequently, an increased addition of fibres caused a reduction in the compressive strength of the composites. For 20% added cellulose, the compressive strength of mortars decreased by 26% (CP), 32% (CRIC) and 46% (CREC) compared to REF (Fig. 5b and c). The addition of fibres, by inducing more voids, lightens and weakens the material (Bentchikou et al., 2012). Anyway, at the 20% fibres addition, the residual R_c was most elevated in CREC mortar

probably due to the best adhesion of the binder paste on CREC fibres as highlighted in the SEM observations (Table 2).

Usually fibres improve the flexural behaviour of mortars thanks to the bridging effect that increases the resistance to crack propagation of brittle matrices (Wang et al., 2000; Aly et al., 2008). However, in this study, the addition of cellulose fibres reduced the binder content and also lightened and increased the porosity and therefore caused weakening of the composite. For these reasons, despite of the fibre type, a beneficial effect in terms of R_f was found until 10% of fibres addition (Fig. 5-c) when the bridging effect overcomes the weakening effect. At higher dosages of CP and CRIC, R_f started to decrease and at 20% of cellulosic addition become comparable (CRIC) or even lower (CP) compared to REF.

Differently, despite the reduction in density and in R_c values, the flexural strength always increased with fibre additions up to 200% at 20% of cellulose addition for CREC mortars (Fig. 5-c). This result was due to their higher aspect ratio and to better adherence between the binder paste and CREC fibres compared to CRIC and CP fibres, as already observed and discussed in Sections 3.3.1. and 3.3.2., respectively. In fact, higher aspect ratio and higher adherence of fibres usually enhance their bridging effect against cracks propagation in mortars.

3.3.2.2. Hygrometric behaviour: Water vapor permeability and moisture buffering capacity. Reduced water vapor permeability is a neg-

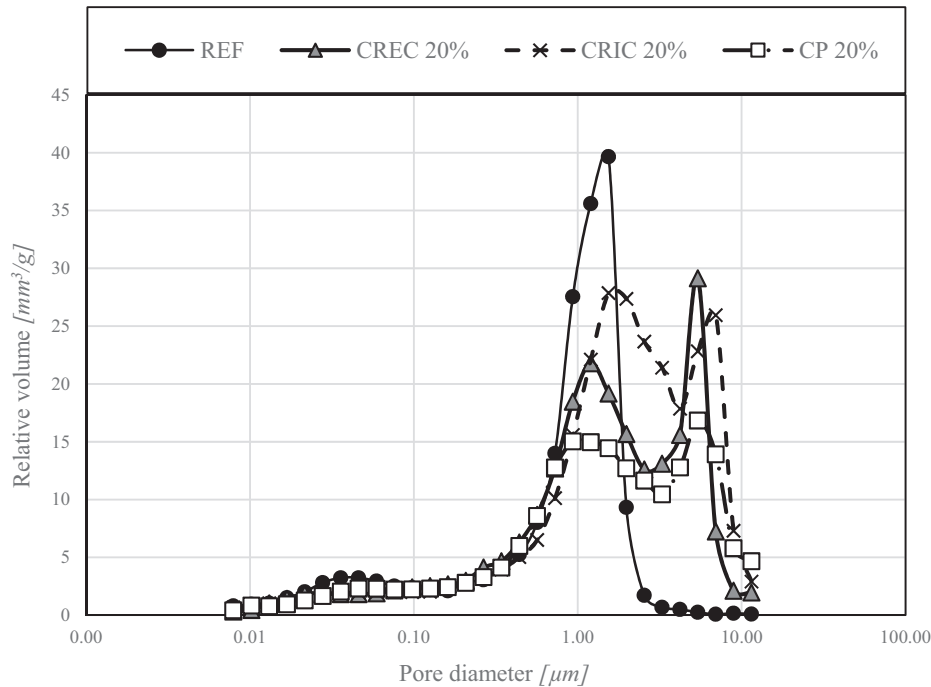


Fig. 4. Pore size distribution of mortars with 0% and 20% addition of cellulose fibres.

ative factor in mortars since it does not allow proper drying of penetrating water and impairs the elimination of water vapor that occurs within buildings. In Table 3 water vapor resistance factor (μ) of all the mixes was presented: REF had the highest value of μ and the addition of cellulose fibres slightly decreased the μ of mortars. A low value of μ indicates higher values of permeability. The cellulose fibres addition in mortar implied an increase in critical pore size and in total open porosity. According to Poiseuille's law, permeability depends on open porosity and on connected pores size (Mobili et al., 2016). For these reasons, the most permeable mix was CRIC 20%, that had the highest open porosity and shifted to the highest diameters.

The higher transpiration of mortar implies a higher moisture penetration depth (Latif et al., 2015) with higher MBV (Giosuè et al., 2016). The more elevated MBV improves the human health in indoor applications. MBV of mortars increases with hygroscopic materials as those cellulose based (Abadie and Mendonça, 2009; Latif et al., 2015). Regardless the type of cellulose fibres considered in this study, the MBV of mortars slightly increased upon their addition. This aspect was verified especially for CREC mortars (Table 3) probably due to their higher affinity to water compared to CP and CRIC fibres characterized by lower wetting ability, as discussed in Section 3.3.2.

3.4. Sustainability and assessment of cellulose recovery

In the last years, the recovery and reuse of cellulosic material interest new and emerging economic sectors. In general, 9 categories of cellulose-based products could be identified as textile, non-woven, wood and timber, pulp/paper and board, cellulose dissolving pulp, cellulosic films, building materials, cellulosic fibre composites and green chemicals (Keijsers et al. 2013). Considering the characteristics of the cellulose in the wastewater and the market possibilities, fine sieved fraction separated by dynamic filter represents an innovative opportunity (Akyol et al., 2019). Several international projects were developed in this direction highlighting that the fine-screening of influent would provide specific oper-

ative cost of 53 W/m³ with significant positive contribution to WWTPs processes further along the treatment chain by making wastewater treatment more efficient and result in a product (mainly cellulose) that could be recovered and valorized (i.e. EU Screencap (screencap.eu), H2020 SMART-Plant (smart-plant.eu)). The recovered cellulose can be used as raw material for new paper products, adhesion binders for asphalts or as fibrous reinforcement material in bricks after properly separation and refining (Crutchik et al., 2018; Kim et al., 2017; Keijsers et al., 2013). The use of natural fibres as the adsorbent is another emerging trend in environmental engineering (Carpenter et al., 2015). However, the choice of the specific applications and the recovery market sectors request inlet materials with diverse standards based on the available amounts and the final productive application. Therefore, the sustainability of the recovery needs to be supported both by global mass balance of the recovered potentiality and by functional tests for the final reuse.

In this study, the experimental results showed that CP fibres can be replaced by CREC fibres in mortars improving their lightweight, flexural behavior and hygrometric properties. The sustainability of the mass balance is demonstrated. In fact, The CREC fibres production was experimentally determined and fitted in Eq. (3). In fact, considering 60% of TSS removal at the optimal SLR (Fig. 3), the Y_{cell} could be predicted equal to 9.2 g of cellulosic material for m³ of influent wastewater. Indeed, in a territorial application with medium size WWTP (50.000 PE) and large size WWTP (150.000 PE), the recoverable theoretical material is estimated to be in the range from 110 kg per day to 331 kg per day, respectively. To obtain 1 ton of mortar with 5% of cellulose fibres by volume, 7.80 kg of CP, 6.18 kg of CRIC and 5.82 kg of CREC are needed. From this point of view, a hypothetical medium size WWTP (50.000 PE) plant could supply a daily production from 102 to 356 sacks per day of pre-mixed mortar with respectively 20% and 5% of REC fibres by volume; whereas a large size WWTP (150.000 PE) plant from 305 to 1069 sacks per day, respectively. Referring to a small-medium company producing cementitious products, (i.e. Diasen srl, Sassoferrato, AN, Italy), 800 sacks per day of 25 kg pre-mixed mortar are produced, satisfying the sustainability of the request compared to the recovery yield.

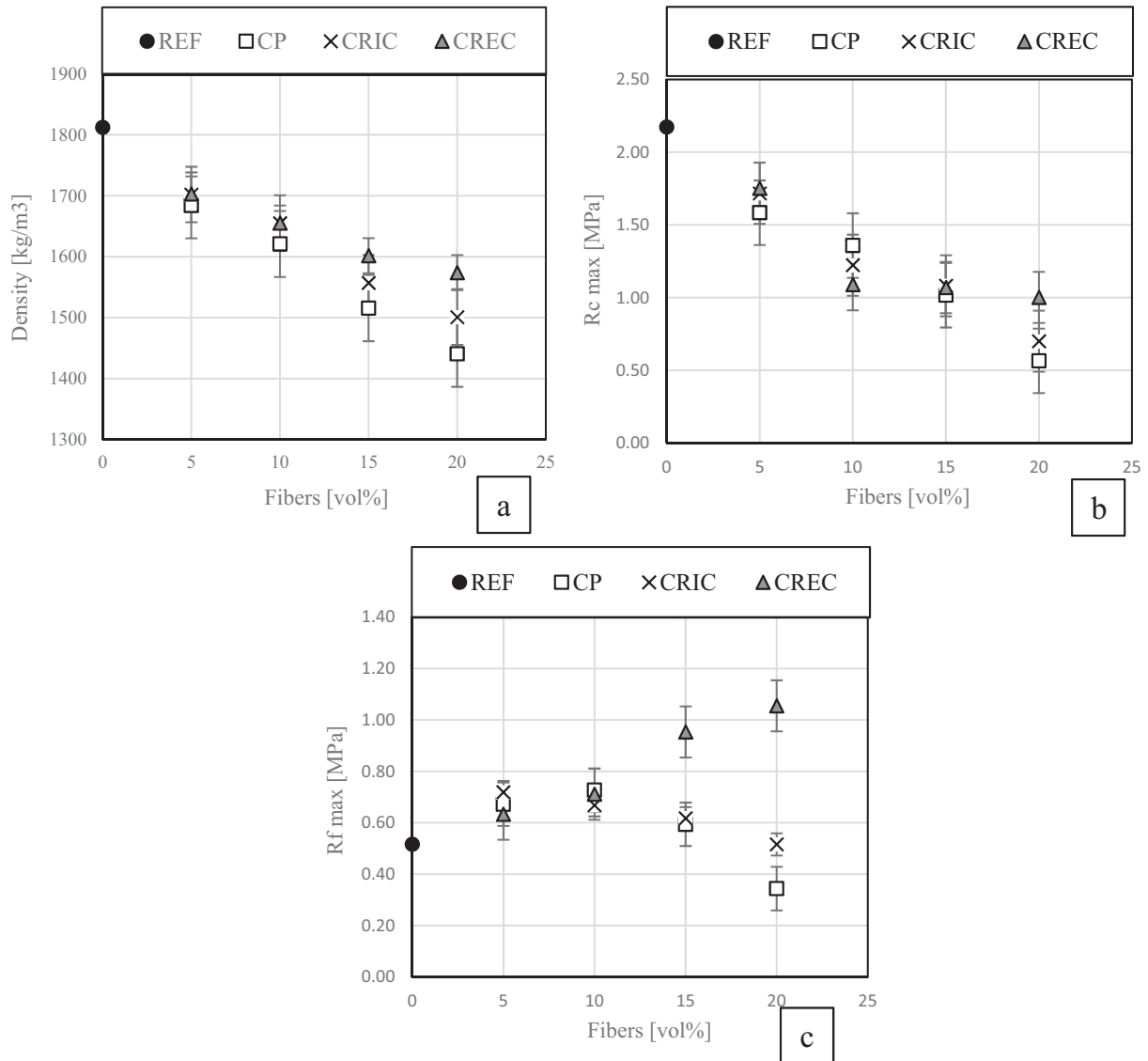


Fig. 5. (a) Density, (b) Compressive strength (Rc) and (c) Flexural strength (Rf) of different mortars.

Table 3
Comparison of $\bar{\mu}$ and MBV results of different mortars.

Specimen	$\bar{\mu}$	MBV [g/m ² -%UR]
REF	11.2	0.07
CP 5%	11.0	0.11
CP10%	10.9	0.13
CP 15%	10.0	0.13
CP20%	9.5	0.15
CRIC 5%	10.7	0.10
CRIC 10%	10.0	0.11
CRIC 15%	9.9	0.11
CRIC 20%	8.9	0.11
CREC 5%	10.2	0.12
CREC 10%	10.1	0.13
CREC 15%	10.0	0.15
CREC 20%	9.7	0.17

4. Conclusions

RBF is an innovative technology for the wastewater sector that enables to enhance solids separation and cellulosic material recovery. The experimental tests in Falconara and Carbonera WWTPs highlighted TSS removal efficiencies between 11% and 74% at SLRs

ranging from 6 kgTS m⁻²h⁻¹ to 108 kgTS m⁻²h⁻¹. These efficiencies allowed to obtain a cellulosic sludge with an average value of Y_{cell} of 0.83 ± 0.14 g cellulosic material per g TS. Analysis of the cellulosic material in the sludge produced by the RBF led to determine the specific cellulosic material production and showed that this matrix is averagely composed of $9 \pm 2\%$ hemicellulose, $38 \pm 6\%$ pure cellulose and $40 \pm 3\%$ lignin and humic compounds.

Y_{cell} was detected equal to 7.82 ± 6.87 g cellulosic material m⁻³, reaching up to 26.6 g cellulosic material m⁻³. All the data collected from experimental tests allowed to obtain a prediction equation that was used to estimate the recovery production of cellulosic material to support the economic assessment for building sector.

To investigate the possibility of valorizing CREC coming from RBF of municipal wastewater in the building sector, CREC fibres were characterized and added in hydraulic lime-based mortars at the amount of 0%-5%-10%-15%-20% by volume. Meanwhile, the properties of mortars manufactured with the same dosages of CP and CRIC fibres were compared. The results showed that the use of CREC fibres in mortars not only allows to valorize a waste but even limits the environmental impact of adding CP fibres.

The obtained results further indicated that CREC fibres, as CP and CRIC fibres, slightly increased the water vapor permeability and the moisture buffering capacity of mortars. This implies an improvement in the human comfort and health if these mortars are applied as renders in indoor applications and a reduction in the use of conventional active systems, as dehumidifiers or air-conditioning systems, which consume energy. As expected, all cellulose fibres, regardless their origin, lightened the mortars and reduced their compressive strength. However, thanks to their higher aspect ratio and better adherence to the binder paste, the residual compressive strength was most elevated in mortars with CREC fibres. Moreover, for the same reasons, the flexural strength increased with the addition of fibres only in mortars with CREC fibres.

Finally, a preliminary balance showed that a large size WWTP (150.000 PE) plant can supply a daily production from 305 to 1069 sacks per day of pre-mixed mortar with 20% and 5% of REC fibres by volume, respectively, that is the average production of a small-medium company producing cementitious products.

Acknowledgements

This study was carried out within the framework of the 'SMART-Plant' Innovation Action which has received funding from the European Union's Horizon 2020 research and innovation program under grant agreement No. 690323. The authors thank to Cir-Tec BV to have provided the tested recovered fibres and to Water Company Vivaservizi to host the University Pilot Hall in Falconara Wastewater Treatment Plant.

References

- Abadie, M.O., Mendonça, K.C., 2009. Moisture performance of building materials: from material characterization to building simulation using the Moisture Buffer Value concept. *Build. Environ.* 44 (2), 388–401. <https://doi.org/10.1016/j.buildenv.2008.03.015>.
- Akyol, Ç., Foglia, A., Ozbayram, E.G., Frison, N., Katsou, E., Eusebi, A.L., Fatone, F., 2019. Validated innovative approaches for energy-efficient resource recovery and re-use from municipal wastewater: from anaerobic treatment systems to a biorefinery concept. *Crit. Rev. Env. Sci. Tec.* 1–34. <https://doi.org/10.1080/10643389.2019.1634456>.
- Aly, T., Sanjayan, J.G., Collins, F., 2008. Effect of polypropylene fibers on shrinkage and cracking of concretes. *Mater. Struct. Constr.* 41 (10), 1741–1753. <https://doi.org/10.1617/s11527-008-9361-2>.
- Andrés, F.N., Beltramini, L.B., Guillarducci, A.G., Romano, M.S., Uliabarie, N.O., 2015. Lightweight concrete: an alternative for recycling cellulose pulp. *Procedia Mater. Sci.* 8, 831–838. <https://doi.org/10.1016/j.mspro.2015.04.142>.
- APHA/AWWA/WEF, 2012. *Standard Methods for the Examination of Water and Wastewater*. 22nd ed. Stand. Methods. Washington, DC, USA. ISBN: 9780875532356.
- Ardanuy, M., Claramunt, J., Toledo Filho, R.D., 2015. Cellulosic fiber reinforced cement-based composites: a review of recent research. *Constr. Build. Mater.* 79, 115–128. <https://doi.org/10.1016/j.conbuildmat.2015.01.035>.
- Ashori, A., Tabarsa, T., Valizadeh, I., 2011. Fiber reinforced cement boards made from recycled newsprint paper. *Mater. Sci. Eng. A* 528 (25–26), 7801–7804. <https://doi.org/10.1016/j.msea.2011.07.005>.
- Behera, C.R., Santoro, D., Germaey, K.V., Sin, G., 2018. Organic carbon recovery modeling for a rotating belt filter and its impact assessment on a plant-wide scale. *Chem. Eng. J.* 334, 1965–1976. <https://doi.org/10.1016/j.cej.2017.11.091>.
- Bentchikou, M., Guidoum, A., Scrivener, K., Silhadi, K., Hanini, S., 2012. Effect of recycled cellulose fibres on the properties of lightweight cement composite matrix. *Constr. Build. Mater.* 34, 451–456. <https://doi.org/10.1016/j.conbuildmat.2012.02.097>.
- Carpenter, A.W., de Lannoy, C.F., Wiesner, M.R., 2015. Cellulose nanomaterials in water treatment technologies. *Environ. Sci. Technol.* 49 (9), 5277–5287. <https://doi.org/10.1021/es506351r>.
- Collet, F., Bart, M., Serres, L., Miriel, J., 2008. Porous structure and water vapour sorption of hemp-based materials. *Constr. Build. Mater.* 22 (6), 1271–1280. <https://doi.org/10.1016/j.conbuildmat.2007.01.018>.
- Collet, F., Pretot, S., 2012. Experimental investigation of moisture buffering capacity of sprayed hemp concrete. *Constr. Build. Mater.* 36, 58–65. <https://doi.org/10.1016/j.conbuildmat.2012.04.139>.
- Crutchik, D., Frison, N., Eusebi, A.L., Fatone, F., 2018. Biorefinery of cellulosic primary sludge towards targeted Short Chain Fatty Acids, phosphorus and methane recovery. *Water Res.* 136, 112–119. <https://doi.org/10.1016/j.watres.2018.02.047>.
- Di Bitonto, L., Lopez, A., Mascolo, G., Mininni, G., Pastore, C., 2016. Efficient solvent-less separation of lipids from municipal wet sewage scum and their sustainable conversion into biodiesel. *Renew. Energy* 90, 55–61. <https://doi.org/10.1016/j.renene.2015.12.049>.
- Dittenber, D.B., Gangarao, H.V.S., 2012. Critical review of recent publications on use of natural composites in infrastructure. *Compos. Part A: Appl. Sci. Manuf.* 43 (8), 1419–1429. <https://doi.org/10.1016/j.compositesa.2011.11.019>.
- Fan, M., Fu, F., 2016. *Advanced High Strength Natural Fibre Composites in Construction*. Woodhead Publishing, Oxford, UK. ISBN:9780081004111.
- Franchi, A., Santoro, D., 2015. Current status of the rotating belt filtration (RBF) technology for municipal wastewater treatment. *Water Pract. Technol.* 10 (2), 319. <https://doi.org/10.2166/wpt.2015.038>.
- Giosuè, C., Mobili, A., Toscano, G., Ruello, M.L., Tittarelli, F., 2016. Effect of biomass waste materials as unconventional aggregates in multifunctional mortars for indoor application. *Proc. Eng.* 161, 655–659. <https://doi.org/10.1016/j.proeng.2016.08.724>.
- Giosuè, C., Pierpaoli, M., Mobili, A., Ruello, M., Tittarelli, F., 2017. Influence of binders and lightweight aggregates on the properties of cementitious mortars: from traditional requirements to indoor air quality improvement. *Mater. (Basel)* 10 (8), 978. <https://doi.org/10.3390/ma10080978>.
- Gómez Hoyos, C., Cristia, E., Vázquez, A., 2013. Effect of cellulose microcrystalline particles on properties of cement based composites. *Mater. Des.* 51, 810–818. <https://doi.org/10.1016/j.matdes.2013.04.060>.
- Gonçalves, H., Gonçalves, B., Silva, L., Raupp-Pereira, F., Senff, L., Labrincha, J.A., 2014. Development of porogene-containing mortars for levelling the indoor ambient moisture. *Ceram. Int.* 40 (10), 15489–15495. <https://doi.org/10.1016/j.ceramint.2014.07.010>.
- Hietala, M., Varrio, K., Berglund, L., Soini, J., Oksman, K., 2018. Potential of municipal solid waste paper as raw material for production of cellulose nanofibres. *Waste Manag.* 80, 319–326. <https://doi.org/10.1016/j.wasman.2018.09.033>.
- Hospodarova, V., Stevulova, N., Briancin, J., Kostelanska, K., 2018. Investigation of waste paper cellulosic fibers utilization into cement based building materials. *Buildings* 8 (3), 43. <https://doi.org/10.3390/buildings8030043>.
- Howard, R.C., Bichard, W., 1992. The basic effects of recycling on pulp properties. *MRS Proc.* 266. <https://doi.org/10.1557/proc-266-195>.
- Huber, T., Kuckhoff, B., Gries, T., Veit, D., Pang, S., Graupner, N., et al., 2014. Three-dimensional braiding of continuous regenerated cellulose fibres. *J. Ind. Text.* 45 (5), 707–715. <https://doi.org/10.1177/1528083714540695>.
- Huber, T., Müssig, J., Curnow, O., Pang, S., Bickerton, S., Staiger, M.P., 2011. A critical review of all-cellulose composites. *J. Mater. Sci.* 47 (3), 1171–1186. <https://doi.org/10.1007/s10853-011-5774-3>.
- Incover Project (Innovative Eco-Technologies for Resource Recovery from Wastewater, n° 689242).
- Industrial Shredders, 2018. URL www.industrialshredders.com.pdf (accessed 21.11.18).
- Jeihanipour, A., Karimi, K., Niklasson, C., Taherzadeh, M.J., 2010. A novel process for ethanol or biogas production from cellulose in blended-fibers waste textiles. *Waste Manag.* 30 (12), 2504–2509. <https://doi.org/10.1016/j.wasman.2010.06.026>.
- Jongvisuttisun, P., Negrello, C., Kurtis, K.E., 2013. Effect of processing variables on efficiency of eucalyptus pulps for internal curing. *Cem. Concr. Compos.* 37, 126–135. <https://doi.org/10.1016/j.cemconcomp.2012.11.006>.
- Kawashima, S., Shah, S.P., 2011. Early-age autogenous and drying shrinkage behavior of cellulose fiber-reinforced cementitious materials. *Cem. Concr. Compos.* 33 (2), 201–208. <https://doi.org/10.1016/j.cemconcomp.2010.10.018>.
- Keijsers, E.R.P., Yilmaz, G., van Dam, J.E.G., 2013. The cellulose resource matrix. *Carbohydr. Polym.* 93 (1), 9–21. <https://doi.org/10.1016/j.carbpol.2012.08.110>.
- Khedari, J., Suttisonk, B., Pratinthong, N., Hirunlabh, J., 2001. New lightweight composite construction materials with low thermal conductivity. *Cem. Concr. Compos.* 23 (1), 65–70. [https://doi.org/10.1016/s0958-9465\(00\)00072-x](https://doi.org/10.1016/s0958-9465(00)00072-x).
- Kim, M., Lee, E.K., Choi, C.J., et al., 2017. Brick insulation composite and method for manufacturing same. *US Pat* 2017 (0191264), A1.
- Latif, E., Lawrence, M., Shea, A., Walker, P., 2015. Moisture buffer potential of experimental wall assemblies incorporating formulated hemp-lime. *Build. Environ.* 93, 199–209. <https://doi.org/10.1016/j.buildenv.2015.07.011>.
- Lucas, S.S., Ferreira, V.M., de Aguiar, J.L.B., 2013. Incorporation of titanium dioxide nanoparticles in mortars—influence of microstructure in the hardened state properties and photocatalytic activity. *Cem. Concr. Res.* 43, 112–120. <https://doi.org/10.1016/j.cemconres.2012.09.007>.
- Maslinda, A.B., Abdul Majid, M.S., Ridzuan, M.J.M., Afendi, M., Gibson, A.G., 2017. Effect of water absorption on the mechanical properties of hybrid interwoven cellulosic-cellulosic fibre reinforced epoxy composites. *Compos. Struct.* 167, 227–237. <https://doi.org/10.1016/j.compstruct.2017.02.023>.
- Matters of Scale – Into the Toilet | Worldwatch Institute, 2018. URL <http://www.worldwatch.org/node/5142> (accessed 12.11.18).
- Mazhoud, B., Collet, F., Pretot, S., Chamoin, J., 2016. Hygric and thermal properties of hemp-lime plasters. *Build. Environ.* 96, 206–216. <https://doi.org/10.1016/j.buildenv.2015.11.013>.
- Mobili, A., Belli, A., Giosuè, C., Bellezze, T., Tittarelli, F., 2016. Metakaolin and fly ash alkali-activated mortars compared with cementitious mortars at the same strength class. *Cem. Concr. Res.* 88, 198–210. <https://doi.org/10.1016/j.cemconres.2016.07.004>.
- Oksanen, T., Buchert, J., Viikari, L., 1997. The role of hemicelluloses in the hornification of bleached kraft pulps. *Holzforschung* 51 (4), 355–360. <https://doi.org/10.1515/hfsg.1997.51.4.355>.

- Osanyintola, O.F., Simonson, C.J., 2006. Moisture buffering capacity of hygroscopic building materials: experimental facilities and energy impact. *Energy Build.* 38 (10), 1270–1282. <https://doi.org/10.1016/j.enbuild.2006.03.026>.
- Pioneer_STP Project (The potential of innovative Technologies to improve sustainability of sewage treatment plants, WaterJPI-JC-2015-10, ID199).
- Project (RESources from URban Blo-waSte, n°730349).
- Rode, C., Peuhkuri, R., Time, B., Svennberg, K., Ojanen, T., 2007. Moisture buffer value of building materials. *J. ASTM Int.* 4 (5), 1–12. <https://doi.org/10.1520/JAI100369>.
- Ruiken, C.J., Breuer, G., Klaversma, E., Santiago, T., van Loosdrecht, M.C.M., 2013. Sieving wastewater – cellulose recovery, economic and energy evaluation. *Water Res.* 47 (1), 43–48. <https://doi.org/10.1016/j.watres.2012.08.023>.
- Savastano, H., Agopyan, V., 1999. Transition zone studies of vegetable fibre-cement paste composites. *Cem. Concr. Compos.* 21 (1), 49–57. [https://doi.org/10.1016/S0958-9465\(98\)00038-9](https://doi.org/10.1016/S0958-9465(98)00038-9).
- Schreck, M., Wagner, J., 2017. Incentivizing secondary raw material markets for sustainable waste management. *Waste Manag.* 67, 354–359. <https://doi.org/10.1016/j.wasman.2017.05.036>.
- Screenap Project (Finescreen supported biological wastewater treatment to enhance plant capacity, Co-funded by the Eco-innovation Initiative of the European Union, ECO/13/630492).
- Shi, S., Zhang, M., Ling, C., Hou, W., Yan, Z., 2018. Extraction and characterization of microcrystalline cellulose from waste cotton fabrics via hydrothermal method. *Waste Manag.* 82, 139–146. <https://doi.org/10.1016/j.wasman.2018.10.023>.
- Silva, A., Rosano, M., Stocker, L., Gorissen, L., 2017. From waste to sustainable materials management: three case studies of the transition journey. *Waste Manag.* 61, 547–557. <https://doi.org/10.1016/j.wasman.2016.11.038>.
- Slanina, P., Šilarová, Š., 2009. Moisture transport through perforated vapour retarders. *Build. Environ.* 44 (8), 1617–1626. <https://doi.org/10.1016/j.buildenv.2008.10.006>.
- SMART-Plant Project (Scale-up of low-carbon footprint MATERIAL Recovery Techniques in existing wastewater treatment PLANTS, n°690323).
- Southeast Green – Business depends on the environment and the environment depends on business. How Much Toilet Paper Is Used Per Year?, 2018. URL <http://www.southeastgreen.com/index.php/seg-features/tips-a-faqs/tips-to-green-your738life/10551-how-much-toilet-paper-is-used-per-year> (accessed 01.12.18).
- Toilet Paper History, 2018. URL <http://www.toiletpaperhistory.net/> (accessed 21.11.18).
- Tran Le, A.D., Maalouf, C., Mai, T.H., Wurtz, E., Collet, F., 2010. Transient hygrothermal behaviour of a hemp concrete building envelope. *Energy Build.* 42 (10), 1797–1806. <https://doi.org/10.1016/j.enbuild.2010.05.016>.
- Triantafyllou G., Přikryl R. Markopoulos T., 2011. Reactivity of hydraulic lime binders: a proposed laboratory testing technique. 13, 7424–7424.
- Válek, J., van Halem, E., Viani, A., Pérez-Estébanez, M., Ševčík, R., Šašek, P., 2014. Determination of optimal burning temperature ranges for production of natural hydraulic limes. *Constr. Build. Mater.* 66, 771–780. <https://doi.org/10.1016/j.conbuildmat.2014.06.015>.
- Van Loosdrecht, M.C.M., Nielsen, P.H., Lopez-Vazquez, C.M., Brdjanovic, D., 2016. *Experimental Methods in Wastewater Treatment*. IWA Publishing, London, UK.
- Wang, Y., Wu, H.C., Li, V.C., 2000. Concrete reinforcement with recycled fibers. *J. Mater. Civ. Eng.* 12 (4), 314–319. [https://doi.org/10.1061/\(asce\)0899-1561\(2000\)12:4\(314\)](https://doi.org/10.1061/(asce)0899-1561(2000)12:4(314)).
- Wei, S., Jiang, Z., Liu, H., Zhou, D., Sanchez-Silva, M., 2013. Microbiologically induced deterioration of concrete: a review. *Brazilian J. Microbiol.* 44 (4), 1001–1007. <https://doi.org/10.1590/s1517-83822014005000006>.
- Wistara, N., Young, R.A., 1999. Properties and treatments of pulps from recycled paper. Part I. Physical and chemical properties of pulps. *Cellulose* 6 (4), 291–324. <https://doi.org/10.1023/a:1009221125962>.
- Zhang, L., Loh, K.C., Zhang, J., 2018. Food waste enhanced anaerobic digestion of biologically pretreated yard waste: analysis of cellulose crystallinity and microbial communities. *Waste Manag.* 79, 109–119. <https://doi.org/10.1016/j.wasman.2018.07.036>.